UiT The Arctic University of Norway

Faculty of Biosciences, Fisheries and Economics, Department of Arctic and Marine Biology

Fibroblast *in vitro* stimulation with TGFβ1 and bFGF

αSMA expression and S100A4 immunohistochemistry staining in oral cancer

Eirini Alexopoulou

BIO-3950 Master`s thesis in Biology, December 2020

Acknowledgements

To begin my acknowledgements, I want to thank the Arctic University of Norway (UiT) as well as the Department of Arctic Marine Biology and Department of Medical Biology for providing the facilities and equipment required to complete this project.

In this present thesis I would like to thank primarily my supervisor Synnøve Magnussen for her precious assistance in supervision of my thesis and her support at any level throughout the research and writing processes of this project. The guidance, patience and knowledge I received enriched my scientific understanding and helped me develop both as a human and a scientist.

My thesis was conducted at the Department of Medical Biology (UiT) in the facilities of tumor biology research group. I would like to express my gratitude for all the staff members in the lab, professors, and colleagues for sharing with me their expertise and precious advices to improve and overcome troubleshooting along my research.

Furthermore, I am thankful to all my professors at Department of Arctic and Marine Biology, where I am registered at, for their patience, understanding, cooperation and help to give me the chance to work on this project and support the collaboration between the two departments.

In these challenging times, I would like to pay special thanks to my support system consisting of my mother, father, siblings and further family, my friends, my partner and my cat for supporting me in various ways on my way to complete my studies. This project has been very challenging, and their contribution was crucial to keep me motivated during my whole master's journey.

Additionally, I would like to thank a few special people like Gerit for her encouragement and academic help as well as Line for her constant support and motivation in the hardest of times. Last but not least, I want to thank Monica Alterskjær Sundset for her precious contribution into the last stages of my thesis writing.

Abbreviations

αSMA – alpha smooth muscle actin
bFGF – Basic fibroblast growth factor
BSA - Bovine serum albumin
CAFs – Cancer associated fibroblasts
DAB - 3,3′-Diaminobenzidine
DPX - Dibutylphthalate polystyrene xylene
ECM – Extracellular matrix
EDTA - Ethylenediaminetetraacetic acid
EGF - Epidermal growth factor
EMT – Epithelial to mesenchymal transition
FAP – Fibroblast activation protein
FBS - Fetal bovine serum
GDF15 - Growth/differentiation factor 15
GLOBOCAN - Global Cancer Observatory
HRP - horseradish peroxidase
IHC - Immunohistochemistry
IL-10 - Interleukin 10
IL-8 - Interleukin 8
MEM – Minimal essential medium
MMPs - Matrix metalloproteases
MPs – metalloproteases
NCAM - Neural cell adhesion molecule
NCI – National Cancer Institute
NFs – Normal fibroblasts
OSCC – Oral squamous cell carcinoma
PBS - Phosphate buffered saline
PDGF - Platelet-derived growth factor
Penstrep - Penicillin-streptomycin solution
PVDF - Polyvinylidene fluoride or polyvinylidene difluoride
RIPA - Radio-Immunoprecipitation Assay
S100A4/FSP1 – S100 calcium binding protein A4 also known as specific fibroblast protein 1
SEER - Surveillance, Epidemiology and End Results program
TAM – Tumor associated macrophages
TBS - Tris-buffered saline
TGFβ1 – Transforming growth factor β1
TME – Tumor microenvironment
Wnt - Wingless-related integration site
ZEB 1/2 - Zinc finger E‑box binding protein 1

Abstract

Oral squamous cell carcinoma (OSCC) is an aggressive cancer associated with high mortality rates. The objective of this master project was to test the following hypotheses: (1) transforming growth factor β1 (TGFβ1) activates fibroblasts *in vitro and* basic fibroblast growth factor (bFGF) deactivates them while both increase fibroblast proliferation in cancer associated fibroblasts (CAFs); (2) the expression of anti-smooth muscle actin (αSMA) increases in presence of TGFβ1 and decreases upon treatment with bFGF; and (3) the calcium binding protein S100A4, also known as specific fibroblast protein 1 (FSP1), is a reliable epithelial to mesenchymal transition (EMT) biomarker for OSCC. A fibroblast cell line (MRC5) was treated with TGFβ1 (2 ng/ml) and bFGF (1, 10 and 100 ng/ml) to examine the effects on fibroblast morphology and proliferation. The impact of TGFβ1 and bFGF treatments on αSMA expression was tested through Western Blot analysis. The accuracy of S100A4 as an OSCC biomarker was tested through immunohistochemistry (IHC) staining on mouse tongue tissues with tumor as literature suggests that in invasive OSCC, S100A4 appears to be overexpressed. The fibroblast cell line was stimulated with TGFβ1 and bFGF which both increased proliferation. TGFβ1 resulted successfully in activated fibroblast morphology with dense fiber formation. Supplementing the microscopy observation, total protein quantification, showed that TGFβ1 treated fibroblasts, had higher total protein content than untreated fibroblasts for all incubations (24, 48 and 72h). For bFGF treated fibroblasts, the average total protein content displayed higher values than controls in all incubations, however, the treated groups had very similar total protein content despite the bFGF treatment concentration. TGFβ1 group was expected to enhance αSMA expression with inconclusive results and bFGF treated cells presented a reduction of αSMA expression compared to the negative control, in agreement with literature references. There was no noticeable variation on αSMA expression among the different bFGF treatments, indicating that bFGF indeed reduces the expression of αSMA, without a bFGF concentration-dependent effect. The S100A4 staining experiment conducted on mouse tongue tissues with tumor and the results seemed to be unclear as S100A4 displayed a lot of staining in various areas outside of the tumor. The positive stains outside of the tumor could be related to other cell types than cancer cells, like fibroblasts, but due to heavy staining it was not possible to identify the cell types and attribute the out-of-tumor locations that correspond to cancer cells. Hence, S100A4 is not a very sensitive biomarker for S100A4.

Table of Contents

1 Introduction

1.1 Epidemiology of oral cancers and oral squamous cell carcinoma

Oral squamous cell carcinoma (OSCC) is a malignancy affecting the head and neck. The most frequent sites include the oral cavity, palate and floor of the mouth as well as the buccal mucosa. OSCC is an aggressive type of cancer, usually asymptomatic in early stages that usually metastasizes to lymph nodes and is therefore associated with a high mortality rate. Main risk factors that contribute to OSCC and related oral cancers development, are alcohol consumption as well as tobacco use, worldwide (Santos et al., 2016). According to Global Cancer Observatory (GLOBOCAN), for the year 2018 there over 350,000 registered cases of oral and lip cavity cancer as well as 92,887 cases for oropharynx cancer, worldwide. For the same year the mortality cases were estimated at 177,384 and 51,005 cases for those types, respectively. Based on the "Surveillance, Epidemiology and End Results program" (SEER) database of the National Cancer Institute (NCI) the localization of the cancer affects the survival rate. In America, the 5-year survival rate is estimated at 90% for lip cancer, 66% for tongue cancer, 52% for cancer on the floor of the mouth and 59% for cancer on other parts of the mouth. Geographically, oral cancer is a dominant cancer type in Southern Asia, Pacific Islands and Africa. In Sri Lanka and India, oral cancer is the primary cancer related death cause. Although registered oral cancer cases are already high, the incidence of oral cancer shows an increasing rate in the future. Shield et al. (2016) estimate that oral (lip and cavity) as well as pharyngeal cancers incidence will show a 62% increase by the year 2035.

Before describing OSCC further, I will first briefly review commonalities of cancers, e.g. the tumor microenvironment, the role of fibroblasts and growths factors as well as the similarities between cancer and natural processes like wound healing.

1.2 The tumor microenvironment (TME)

The tumor microenvironment (TME) consists mainly of tumor associated macrophages (TAMs), fibroblasts, immune and stromal cells, soluble factors and extracellular matrix (ECM) molecules (Sasahira et al., 2018) and enzymes such as metalloproteases (MPs). The interactions (direct through cell-to-cell contact or indirect through soluble factors) within the TME are crucial for the tumor formation, progression and metastasis. The reason is that the dynamic between the different cell types and proteins can yield both a cancer promotive and immune suppressive outcome, as observed in cancer associated fibroblasts (CAFs)-TAM interaction (Higashino et al., 2019).

1.3 Comparison of wound healing and cancer

Fibroblasts are naturally abundant in tissue stroma and they secrete ECM molecules (Sasahira et al., 2018). Notably, wound healing and cancer development have similar cell / metabolic processes in common. In wound healing but also cancer (and embryogenesis), one of the many processes that takes place is the so called Epithelial to Mesenchymal Transition (EMT). Additionally, activated fibroblasts participate both in wound healing and cancer development. In wound healing they are termed “myofibroblasts” whereas in cancer, they are called “cancer associated fibroblasts”.

The first stage of wound healing (**Figure 1**) is hemostasis and the procedure is similar between wound healing and cancer. Hemostasis aims to prevent bleeding from the wound by keeping the blood in the injured blood vessel. During hemostasis, platelets cluster in a blood clot near the wound and transform into a fiber-like clot, together with fibrin and plasma proteins. Then, a base of the new matrix is formed, consisting of fibrin, fibronectin and vitronectin. That is the point where fibroblasts are recruited to the wound site. Both wound healing and cancer require activated fibroblasts. Activated fibroblasts participate in all three stages of wound healing as they secrete important factors of the new ECM like collagen while contributing to the remodeling of the matrix as well as the contractions of the healing tissue (Desjardins-Park et al., 2018). The main difference between wound healing and cancer formation is that wound healing has an end point whereas cancer formation is indefinite, therefore, cancer doesn’t result in a sealed wound and scar. Inflammation includes the recruitment of macrophages, neutrophils and monocytes in both wound healing and cancer (Foster et al., 2018).

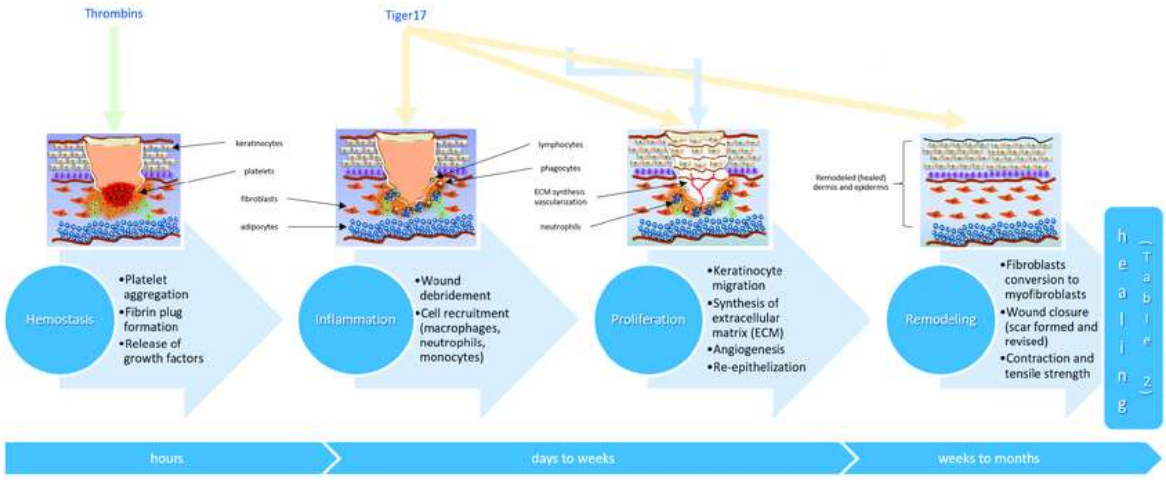

Figure 1. Representation and main stages of wound healing: hemostasis, inflammation, proliferation and tissue remodeling. Hemostasis is driven by the release of growth factors and leads to inflammation state, where macrophages, neutrophils and monocytes are recruited. Proliferation stage follows up, facilitating the migration of keratinocytes. The ECM is synthesized and processes such as angiogenesis and re-epithilization take place. Lastly, tissue remodeling requires the differentiation of fibroblasts into myofibroblasts, the sealing of the wound, the formation of the scar in order to achieve contraction and strengthen the tensile. Some molecules, such as Tiger17 are present in more than one stages whereas other peptides are stage specific. The Figure has been modified and originates from Gomes et al. (2017).

1.4 Activation of fibroblasts

Activation of fibroblasts is a natural procedure and is characterized by the higher expression of α-smooth muscle actin (αSMA) that influences a change in morphology, as well as expression of fibroblast activation protein (FAP) (Sahai et al., 2020). Specifically, for cancer, activated fibroblasts that are present in the TME are termed cancer associated fibroblasts (CAFs). CAFs are highly present in the tumor stroma. Stromal fibroblasts get activated by macrophages and growth factors such as transforming growth factor-β1 (TGF- β1) which promote differentiation of fibroblasts into CAFs. However, the exact mechanism of fibroblast to CAF conversion is unclear due to the heterogeneity of progenitor cells as well as the variety of pathways that lead to the conversion, among different cancer types. For instance, in breast cancer, Notch signaling between cancer cells and fibroblasts result in CAF activation whereas in OSCC, CAF activation is driven by the loss of Notch signaling (Sahai et al., 2020).

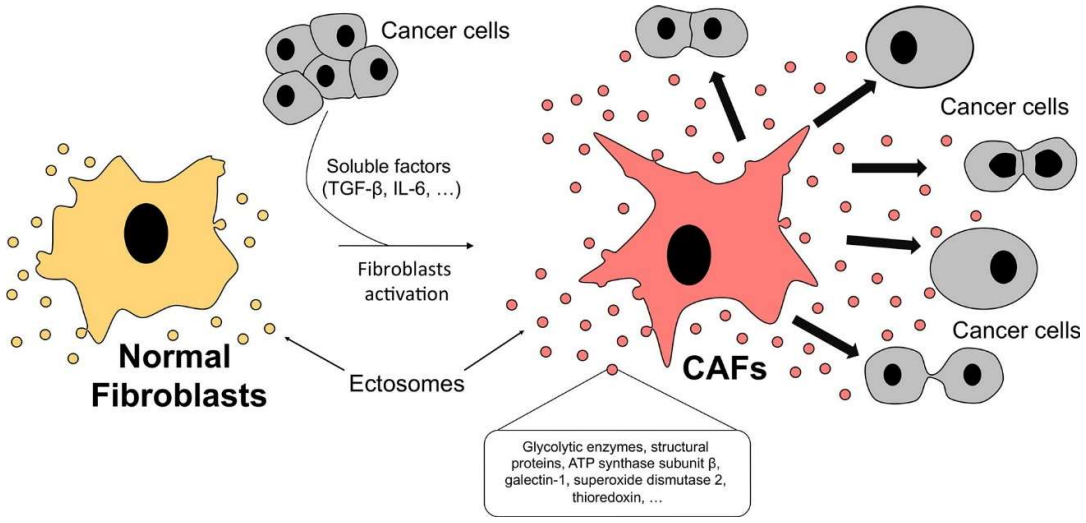

Figure 2. Normal fibroblast activation. Soluble factors such as TGFβ1 stimulate stromal fibroblasts and differentiate them into cancer associated fibroblasts. Proteins secreted by CAFs during the conversion promote the proliferation of cancer cells. Source: Santi et al. (2015).

1.5 Cancer associated fibroblasts (CAFs) and interactions within tumor microenvironment (TME)

CAFs are a very heterogenous cell population since they can originate from various types of progenitor cells. Besides fibroblasts, epithelial cells, endothelial cells, cells within bone marrow and hematopoietic stem cells can all differentiate to CAFs (Higashino et al., 2019). CAFs can initiate tumor growth and sculpt the tumor microenvironment (TME). The transition from normal fibroblast to cancer associated fibroblast is packed with alterations in the protein expression (higher αSMA, production of TGF-β1) as well as in the morphology (increase of actin stress fibers).

CAFs act on tumor cells by secreting proteins that have both a direct and indirect impact on tumor cells. Furthermore, CAFs degrade the ECM through secreting factors which activate stromal cells, as seen in the example of cytokine secretion. Cytokines have the capacity to promote proliferation and migration both on macrophages and tumor cells. Monocytes are recruited into the tumor tissue by CAFs. The tumor microenvironment facilitates the differentiation of monocytes into macrophages. There are two different types, Type M1 and Type M2, with distinct functions as a response to stimulation signals (Lee, 2019). Type M1 macrophages (proinflammatory) are involved in the immune response against viruses and

induce the response of helper T cells against infections. Type M2 (anti-inflammatory) are involved in immune response regulation, tissue repair and tumor promotion. When stimulated by IL-10 and TGFβ, Type M2 macrophages can promote tissue remodeling and become tumor associated macrophages (TAM). When macrophage polarization from type M1 to type M2 takes place, the monocytes induce an upregulation of EMT genes, suppress the epithelial markers (ex. E-cadherin) while upregulating mesenchymal markers (ex. Vimentin) on cancer cells and act as an immune suppressor through the PD-1 axis (Yavuz et al., 2019). The overall immune suppressive environment is enhanced by M2 macrophages. M2 macrophages express proteins like neural cell adhesion molecule (NCAM) that affect cell-to-cell adhesion, growth / differentiation factor 15 (GDF15) that controls growth and differentiation, as well as interleukin IL-8 promotes migration. The immune suppression is further supported by secretion of anti-inflammatory factors (TGFb1, interleukin IL-10) by M2 macrophages. (Yavuz et al., 2019). Thus, Type M2 macrophages can lead to direct tumor progression.

In the case of OSCC, particularly metastasis, the OSCC migrates to cervical lymph nodes through the lymphatic vessels, depending on the location of the primary tumor (Sasahira et al., 2018). Initially, E-cadherin downregulation paired with simultaneous overexpression of integrins, result to cell detachment. Next, MMPs, a family of proteolytic enzymes, facilitate the disruption of basal membrane which in turn, triggers the cell mobility and stromal infiltration. Once the cancer cells have gained mobility, they can either enter the lymphatic or vessel system, migrate in it, exit and form a second tumor in a new site, or locally invade a nearby tissue. The invasive activity is associated with a series of abnormalities such as the expression of critical EMT factors (TGF-β, Wnt, Notch, epidermal growth factor-EGF, platelet-derived growth factor PDGF) as well as mesenchymal factors (αSMA, vimentin, N-cadherin) and additional upregulation of Snail, Slug, TWIST, Zinc finger E‐box binding protein 1 and 2-ZEB1/2 transcriptional factors (Weinberg, 2015).

1.5.1 Transforming growth factor – β1 (TGF-β1)

TGFβ1 is a growth factor, encoded by TGFB1 gene in humans and is secreted by various cell types-fibroblasts included. TGFβ1 is usually inactive. The activation of TGFβ1 pathway is diverse and can sometimes be specific to the cell or tissue type depending on the activation factor. When TGFβ1 is expressed, it forms serine / threonine kinase complexes and then binds to TGFβ1 receptors to get active. Upon activation, TGFβ1 can initiate signaling cascades that induce transcription of genes responsible for cell differentiation, activation of immune cells as

well as release of regulatory proteins. Previous research suggests that TGFβ1 stimulation of fibroblasts in vitro results in increased proliferation and collagen production as well as differentiation. Interestingly enough, this effect is observed both among human (Liu et al., 2016) and cattle (Maroni et al., 2012) fibroblasts. Several studies suggest that CAFs play an important role in progression and invasion of various cancer types, both in human and animal cancer research. The complexity of CAF functions within the TME is an active challenge in research and requires more specific projects to provide an understanding of exactly how the fibroblast behave among different types of cancer.

1.5.2 Basic fibroblast growth factor (bFGF)

Basic fibroblast growth factor (bFGF) in humans is coded by FGF2 gene (Kim, 1998) in chromosome 4 and gets synthesized by fat cells. In normal tissues bFGF is found on the basement membrane and as a part of blood vessel ECM. In the presence of signaling proteins, bFGF induces EMT by downregulating epithelial markers such as E-cadherin while upregulating mesenchymal factors like vimentin. bFGF regulates both proliferation and fibroblast differentiation, especially during wound healing which requires EMT to take place. Upregulation of bFGF under EMT can also alter the phenotype of endothelial cells. Endothelial cells begin to proliferate, construct capillary walls and therefore facilitate angiogenesis (Weinberg, 2015). There is evidence that bFGF regulates the expression of proteolytic enzymes such as collagenases and matrix metalloproteinases (Song et al., 2000) in human breast and colon cancer as well as melanoma. As a result, the disruption of ECM leads to cell motility and migration. Hence, bFGF has the capacity to promote metastasis. All things considered, bFGF role in tumor formation, development, angiogenesis (Nakamichi et al., 2016) and metastasis should be further investigated (Hase et al., 2006).

1.6 CAF markers

1.6.1 alpha smooth muscle actin (αSMA)

In OSCC, there is an abundance of CAFs in the tumor associated stroma. High amounts of alpha smooth muscle actin (αSMA) protein, expressed by (stromal) CAFs, are present in solid OSCC tumors (Elmusrati et al., 2017). Consequently, CAF detection and role is a key-target for OSCC research due to the highly interactive activity and contribution to cancer formation. Since cancer cell proliferation, angiogenesis, inflammation, and metastasis are all stimulated directly or indirectly by CAFs, their presence could play as an indicator for OSCC prognosis

in patients. αSMA is expressed by CAFs and not in normal fibroblasts, therefore, it can be used to detect CAFs, unlike other markers that are not selective (Yavuz et al., 2019).

1.6.2 S100A4

Another EMT biomarker associated to OSCC is the calcium binding protein S100A4 which is also known as specific fibroblast protein 1 (FSP1). S100A4 is a regulator of cell proliferation and tissue remodeling in wound healing or disease (Bussard et al., 2017). Additionally, S100A4 activates EMT by downregulating the basic epithelial marker E-cadherin and is linked to tumor progression when it gets hypermethylated and overexpressed (Sherbet, 2017). S100A4 is expressed in cancer cells, macrophages, fibroblasts and lymphocytes and can act as an indicator for metastasis (Wetting et al., 2011). It is reported that an overexpression of S100A4 is highly linked to lymph node invasion and can act as a predictor of tumor recurrence (Natarajan et al., 2014). Specifically, in metastasis expression of S100A4 promotes cell motility indirectly by loosening the epithelial cell adhesion (due to E-cadherin downregulation) or directly when it interacts with chemoattractants (ex. myosin-IIA) (Li et al., 2006). In addition, S100A4 is also reported to stimulate angiogenesis in other types of cancer (Fei et al., 2020) which highlights the active contribution of S100A4 in cancer progression. The TME also appears to play a crucial role in S100A4 link to cancer, as it induces S100A4 expression in human carcinoma xenograft tumors (Wetting et al., 2011).

2 Aims and hypothesis

In this master thesis, I am going to test three hypotheses:

1) Transforming growth factor beta 1 (TGFβ1) and basic fibroblast growth factor (bFGF) activate fibroblasts *in vitro*, increase proliferation and promote activated fibroblast morphology in cancer associated fibroblasts (CAF)s.
2) The expression of anti-smooth muscle actin (αSMA) increases in presence of TGFβ1 and decreases upon treatment with bFGF.
3) The calcium binding protein S100A4 is a reliable biomarker for oral squamous cell carcinoma.

The objectives of this project are:

1) To test the *in vitro* activation of fibroblasts into CAFS with tumor growth factor beta 1 (TGFβ1) and basic fibroblast growth factor (bFGF) which are both known to increase proliferation. A fibroblast cell line was treated with TGFβ1 and bFGF in order to examine the effects on fibroblast morphology and proliferation.

2) To investigate the impact of TGFβ1 and bFGF treatments on anti-smooth muscle actin (αSMA) expression through Western Blot analysis.
3) To test the accuracy of S100A4 protein as an oral squamous cell carcinoma (OSCC) biomarker through immunohistochemistry (IHC) staining on mouse tongue tissues with tumor as literature suggests that in invasive OSCC, S100A4 appears to be overexpressed (Natarajan et al., 2014).

3 Methods section

3.1 Fibroblast cell line and culture

A MRC5 cell line was used for a series of experiments in this project. MRC5 cells are human lung fibroblasts with an average life span of 42 to 46 divisions according to the vender (ATCC – LGC Standards, Norway). The cells were cultured in Eagle's Minimum Essential Medium (MEM) as recommended by the vender and supplemented with 10% (v/v) fetal bovine serum (FBS) to promote cell growth as well as 1% (v/v) penicillin-streptomycin solution (Penstrep). MRC5 are adherent cells and were cultured at 37^{o}C and 5% CO2.

3.1.1 Passaging cells

Cells were passaged by washing the flask with 5 ml phosphate buffered saline (PBS) in order to remove FBS and ensure that the α1-antitrypsin protease inhibitor which is present in FBS will not disrupt the trypsin activity (Rauch et al., 2011). To achieve cell detachment 1 ml trypsin ethylenediaminetetraacetic acid (EDTA) solution (T4049, Sigma-Aldrich, Germany) was added and incubated for approximately 3 minutes at 37^{o}C. Then, after the cells were detached, 5 ml MEM were added in the cell-trypsin flasks. The mixture then was divided 1:3. For re-culture purposes 2 ml transferred in a new flask with 10 ml MEM, and the excess was used for cell counting and seeding purposes.

3.2 Fibroblast treatment with TGFb1

The purpose of the method was to examine the possibility of *in vitro* fibroblast activation / stimulation with TGFβ1 (Desmoulière et al. 1993; Maroni et al. 2012) in 24, 48 and 72h treatments.

MRC5 cells were seeded 50.000 cells / well in a 12 well plate and incubated for 24 hours. Cells either received 2 ng/ml TGFβ1 or an equal volume of TGFβ1 buffer as a negative control in 1 ml MEM. Each well was washed twice with 1 ml PBS and harvested with radio-immunoprecipitation assay (RIPA) lysis buffer (25nM Tris, 0.15M NaCl, 1% Triton, 1%

SDS, 0.5% NaCl deoxycholate), mixed with (1:100) volume of protease inhibitor. Lastly, the samples were sonicated at 4ºC for 20 cycles (20'' ON, 20'' OFF) and stored in -20ºC.

3.3 Fibroblast Activation with bFGF

This method aims to stimulate fibroblasts *in vitro* with bFGF to observe its impact on αSMA expression since literature suggest a downregulation of αSMA as a response to bFGF treatment. For this experiment, 50.000 cells were seeded in 12 well plate and incubated for 24, 48 and 72h. Cells received bFGF at concentrations of 1 ng/ml, 10 ng/ml and 100 ng/ml in triplicates. Untreated cells (negative controls) were given an equal volume of PBS (P3813, MerckMillipore, Germany) in triplicates/duplicates. PBS volume was equal to the highest concentration treatment. Samples were harvested, sonicated, measured for total protein content and analyzed with Western blot technique.

3.4 Total Protein Quantification

Total protein quantification took place in order to analyze the samples with Western Blot. Sample preparation was achieved with BIORAD DC TM Protein Assay protein measurement kit and total protein was quantified with Softmax Pro 3.0 Software. Bovine serum albumin (BSA) standard protein by PIERCE was used in stock concentration 2 mg/ml to create standard dilutions for protein measurement calibrations in order to estimate the total protein concentration of the samples.

The serial dilutions ranged from 0 to 1.4 μg/ μl. The standard protein was diluted with RIPA lysis buffer. A 96 well plate was loaded with 5 μl of standard protein/sample per well, followed by 25 μl/well of Reagent A (#500-0113, BIORAD, USA) + Reagent S (#500-0115, BIORAD, USA) mix (1000:20) from the kit and topped with 200 μl/well Reagent B (#500-0114, BIORAD, USA). The plate undergone shaking for 15 minutes and then was quantified in VERSAmax tubable microplate reader by Molecular Devices. The software (Softmax Pro 3.0) was adjusted to 750 nm wavelength for the measurements.

3.5 Western Blotting for αSMA expression

Western Blot protocol was used to examine the expression of αSMA protein on TGFβ1 and bFGF treated samples. The samples were diluted in RIPA buffer to reach approximately 15μg of total protein content in 20 μl volume and mixed with 5 μl of 5x loading buffer (0.05M Tris-HCl Ph 6.8, 2% SDS, 10% glycerol, 0.1% bromphenol blue). Additionally, 10 μl biotinylated protein (#7727, Cell Signaling, Europe B.V.) was used as ladder and mixed with 15 μl of 1x

loading buffer. The samples and ladder were boiled to denature the proteins and then loaded on NuPAGE 10% Bis-Tris gel (NP0301BOX, Invitrogen, USA) for electrophoresis at 200V for 35 minutes with SDS running buffer*. The SDS running buffer was prepared with 30 ml 20x SDS (L3771, Sigma-Aldrich, Germany) and 570 ml dH_2O. The PVDF transfer membrane was activated with methanol (200-659-6, Sigma-Aldrich, Germany) for 15 seconds, distilled water (dH_2O) for 1 minute and sank for 25 seconds in blotting buffer. The blotting buffer consisted of tris-base (648310, MerckMillipore, Germany), glycine (G8898, Sigma-Aldrich, Germany), methanol and dH_2O. Sample blotting took place at 25V for 75 minutes.

3.5.1 Ponceau S membrane staining

Membranes were Ponceau S stained in order to evaluate equal protein loading. After blotting, the transfer membrane was washed three times with Tris-buffered saline (TBS) solution for 5 minutes and then reactivated with methanol for 30 seconds, followed up by dH_2O wash for one minute and an additional TBS wash for 5 minutes. Then, Ponceau S was added and incubated for 5 minutes on shaker. Next, the membrane was washed with dH_2O on shaker until bands were visible and imaged before further stain removal wash.

3.5.2 Blocking and Detection

Post blotting, the membrane was blocked with 5% non-fat milk in Tris-buffered saline Tween (TBS(T)) buffer for one hour in order to prevent the unspecific binding of antibodies across the membrane. That way, the visualization of membrane would yield a clearer result without too high background. Next, 5 µl of Rabbit anti smooth muscle actin antibody (1:1000) was added in the blocking buffer and the membrane was incubated overnight at 4ºC on rotation. Afterwards, the membrane was washed 3 times with TBST (5M NaCl, 1M Tris-base, dH_2O, 20% Tween) to wash off the excess protein and then fresh blocking buffer was added along with 5 µl Goat-Anti Rabbit horseradish peroxidase (HRP) antibody and 5 µl Anti-biotin HRP antibody for the ladder for an additional one-hour incubation. Lastly, a three step TBST wash was performed, and the membrane was developed with 1:1 Chemiluminescent peroxidase substrate-3 solution (CPSOC, Sigma-Aldrich, Germany). The membrane was imaged in LAS4000 (Fujifilm, USA) imaging system.

3.6 Immunohistochemistry for S100A4

Immunohistochemistry (IHC) was performed on mouse tongue tumor tissues to visualize S100A4 protein expression and distribution in order to evaluate the S100A4 accuracy as a biomarker for OSCC. The S100A4 antibody (#41532, Abcam, UK) was used for these experiments. Antibody dilutions were tested in a range from (1:50 – 1:3000) for optimal procedures. After optimization, 1:3000 S100A4 primary antibody dilution was chosen for the conduction of this experiment.

Mouse tongue tissues were rehydrated in xylene for 10 minutes, twice. Then, two 5-minute baths in absolute ethanol took place and followed up by two baths in 96% ethanol, again for 5 minutes each. Lastly, the slides were washed in dH_2O for 3 minutes. To block peroxidase activity, tissue sections were incubated with 3 drops of H_2O_2 NAF 3% peroxidase solution (Norges Apotekerforening) per slide. The tissues were incubated for 10 minutes and then undergone a three step PBS wash. Upon washing, 50 µl of blocking solution (1.5% Goat serum by DAKO in PBS) were added on each slide for a 20-minute incubation in room temperature. Afterwards the slides were additionally topped with 50 µl Antibody solution, consisted of Rabbit S100A4 AbI (#41532, Abcam, UK) and blocking solution (1:3000) and incubated overnight at 4 °C.

The mouse tongue tissues were rinsed with dH_2O, washed 3 times with PBS and then 3 drops of secondary HRP antibody were added from the Dako EnVision System-HRP(DAB) kit. After a 30-minute incubation the tongue sections were washed 3 times with PBS and then topped with 50 µl of 3,3′-Diaminobenzidine (DAB) solution per section. Dab solution stayed on the tissues for 10 minutes in room temperature and was then rinsed off, above hypochlorite bath. A three-step water bath followed up to wash off the slides. In conclusion, the tissues were placed in hematoxylin (#6765004, Chemi-Teknik AS, Norway) for 40 seconds, in order to achieve nucleus staining through oxidation of the nuclear histones, resulting in blue color. The slides were then rinsed and further washed three times with H_2O. Right after, the tissues were dipped into Scott′s Tap Water Substitute Concentrate solution (S5134, MerckMillipore, Germany) for 15 seconds in order to enhance the blue color from hematoxylin step and retain as much tissue on the slides as possible. The slides went through a last dH_2O bath and got dehydrated through a sequence of 96% ethanol, absolute ethanol, and xylene baths. Each bath step was performed for 2 minutes, twice. The mouse tongue tissue slides were sealed with Dibutylphthalate polystyrene xylene (DPX) Mountant (44581, Sigma-Aldrich, Germany) for

histology. After the slides were sealed, they were imaged under the microscope (LEICA DM2000) and imaged in 1.6x, 4x and 10x magnification with LASV3.7 software.

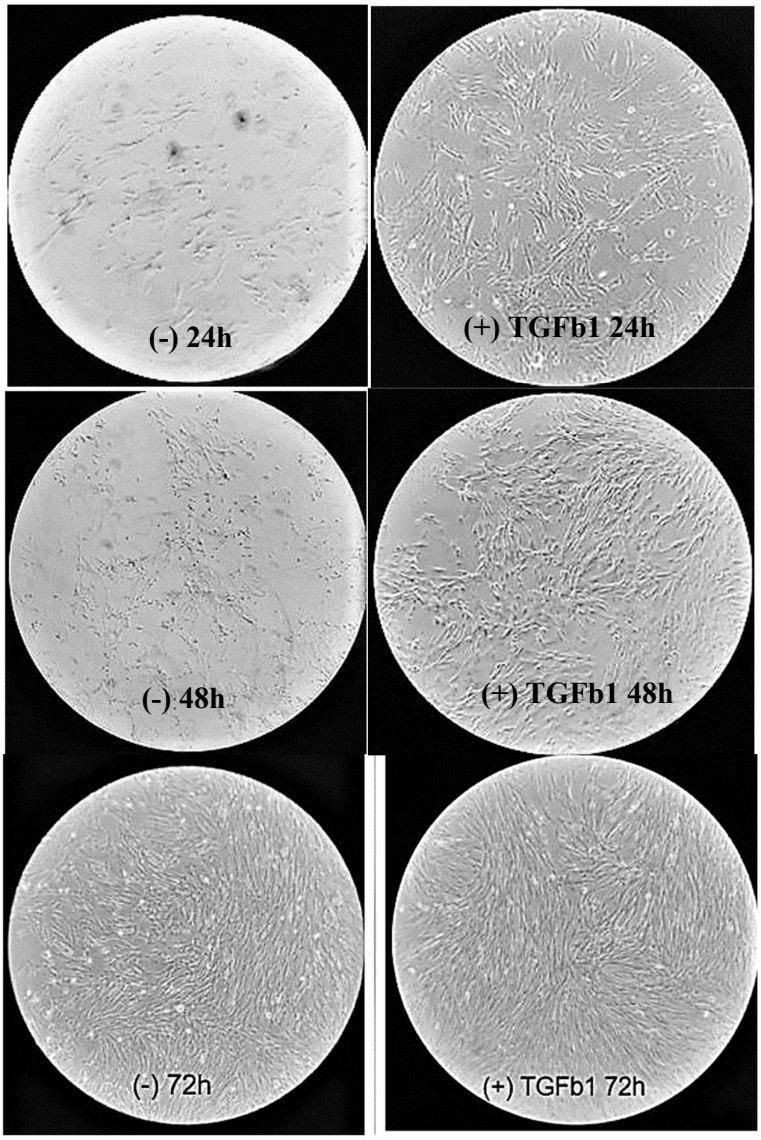

Figure 3. Fibroblast *in vitro* activation with transforming growth factor β1 (TGFβ1). MRC5 cell line on 12 well plates, treated with 2 ng/ml TGFβ1 (right) and incubated for 24, 48 and 72h. Negative controls on the left. At 24 and 48h the treated group proliferated faster and displayed stronger fiber morphology compared to the negative controls. At 72h there was no detectable difference in morphology and proliferation between treated and untreated samples. Pictures captured with external camera through 4x magnification lens, under LEICA DMIRB microscope with LAS 3.7 software.

4 Results

4.1 Fibroblast activation with TGFβ1

Fibroblast treatment with TGFβ1 aimed to examine the impact of TGFβ1 on morphology, as well as to monitor the cell growth. The TGFβ1 fibroblasts were treated with 2 ng/ml as a fixed concentration because TGFβ1 has been reported to enhance proliferation (Liu et al., 2016) and additionally, based on tests that other performed in the same lab, this concentration seems to have an enhancing effect on other cell types. The cells displayed the typical flat, elongated morphology faster compared to the negative control groups (treated only with TGFβ1 buffer) (**Figure 3**). Specifically, at 24h and 48h the treated group appeared to have a more prominent fiber complex phenotype of activated fibroblasts compared to the untreated group as shown in **Figure 3**.

The cells seemed to proliferate faster under TGFβ1 treatment following the literature references on the field. At 72 hours, both treated and untreated cells seemed to be confluent without any noticeable difference.

4.2 Fibroblast stimulation with bFGF

To test the second part of hypothesis 1, we experimented with a range of bFGF concentrations (1-100 ng/ml) and monitored the impact on cell growth and morphology on bFGF treated fibroblasts, for each concentration. The MRC5 cell line was treated with bFGF in concentrations of 1, 10 and 100 ng/ml. Each group was incubated for 24, 48 and 72h. As presented in **Figure 4**, the highest concentration group (100 ng/ml) seems to proliferate faster at 24h compared to the negative controls. At 48 and 72h incubations, the fibroblasts were very dense among all treatment groups therefore there was no visual effect on morphology caused by bFGF for these incubations. At 72 hours, all wells were 100% confluent. The activated fibroblast morphology was weakly present at 24h and became very prominent at 48 and 72h for both negative controls and treated groups. As expected, bFGF seems to have increased proliferation.

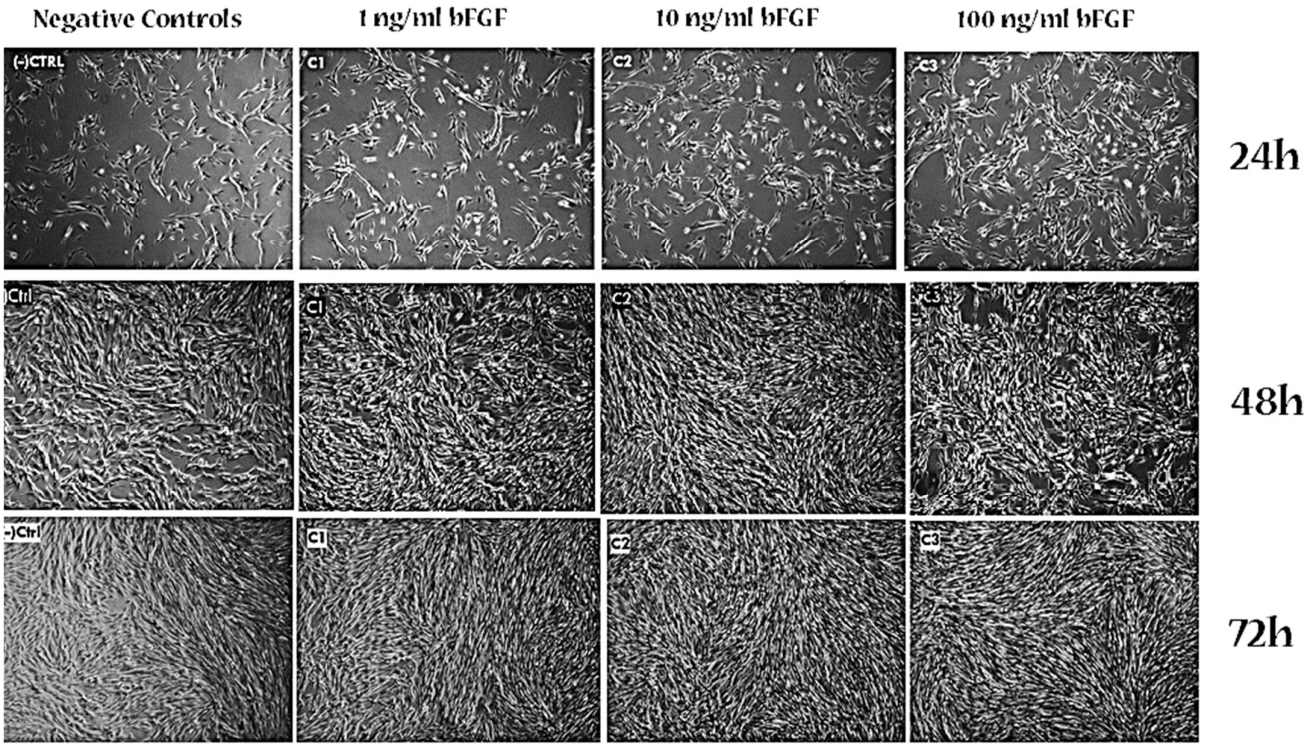

Figure 4. Fibroblast *in vitro* activation with basic fibroblast growth factor (bFGF). Culture pictures of MRC5 cells treated with 1, 10 and 100 ng/ml of bFGF for 24, 48 and 72h. Negative controls at the left column. Pictures are taken under LEICA DMIRB microscope, 4x magnified, with LAS 3.7 software. At 24h, the highest bFGF treated group proliferated faster compared to the negative controls and the cells had more prominent fiber formation. At 48 and 72h all treated groups were very dense and there was no observed difference among the treatments. An increase in proliferation seems to be an effect of bFGF enhancement, particularly the first 24h of treatment.

4.3 Total Protein Quantification

Total protein content was quantified in order to verify the visual proliferation results as well as to calculate the required amount for equal protein load for Western blot analysis. Additionally, total protein quantification provided data for comparison between treated and untreated groups in the pace of 24, 48 and 72 hours.

Upon total protein measurement and analysis, both TGFβ1 (**Figure 5**) and bFGF (**Figure 6**) samples appear to have the lowest total protein content at 24 hours, which kept increasing at 48 hours and reached the highest value at 72 hours. For the TGFβ1 experiment, the negative control group had very similar total protein content compared to the treated group at 24 hours, however, at 48 and 72 hours the TGFβ1 treatment had greater average total protein concentration with smaller standard deviation among the replicates, as shown in **Figure 5**.

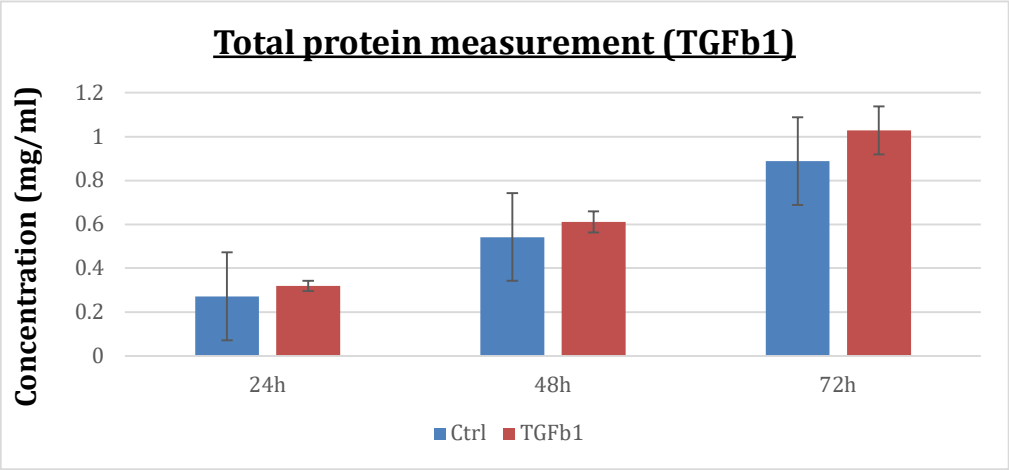

Figure 5. Total Protein Quantification for transforming growth factor-1 (TGFβ1) treated groups, calibrated based on bovine albumin serum (BSA) Standard protein measurement. Original optical density values obtained through VERSAmax tunable microplate reader (Molecular Devices) and Softmax Pro 3.0 software. Microsoft Excel platform was used for data analysis and graph generation. The values correspond to the average sample concentration of each group. The error bars represent the ±standard deviations based on three samples (n=3).

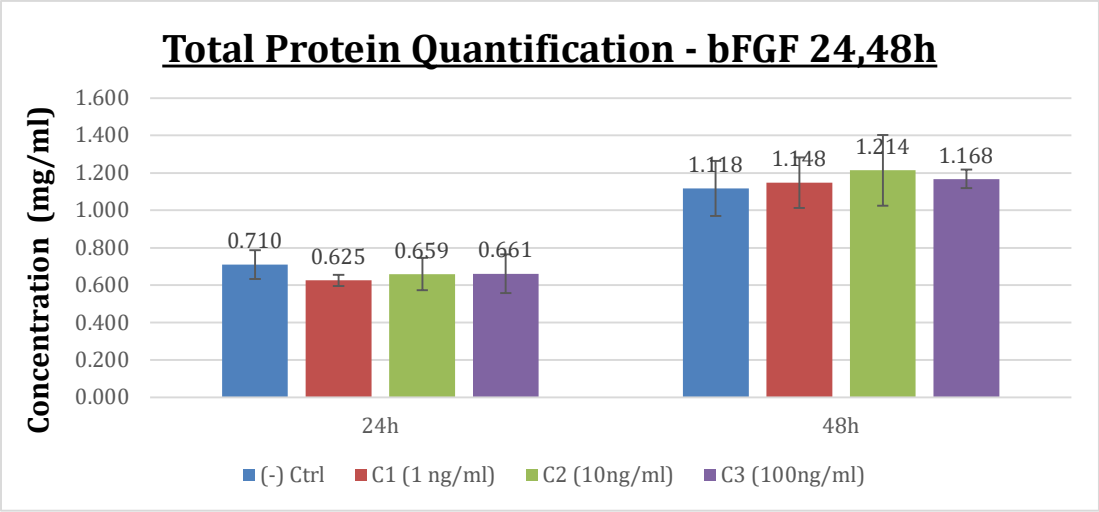

Figure 6. Total protein concentration of negative controls and basic fibroblast growth factor (bFGF) treated groups at 24 and 48 hours. Original optical density values to calculate concentration, obtained through VERSAmax tunable microplate reader (Molecular Devices) and Softmax Pro 3.0 software . Microsoft Excel platform was used for data analysis and graph generation. The graph values correspond to the average total protein concentration of samples for each group. All treated groups displayed similar total protein content, which was higher than the negative controls at 48h. The error bars show the ±standard deviations based on three samples (n=3).

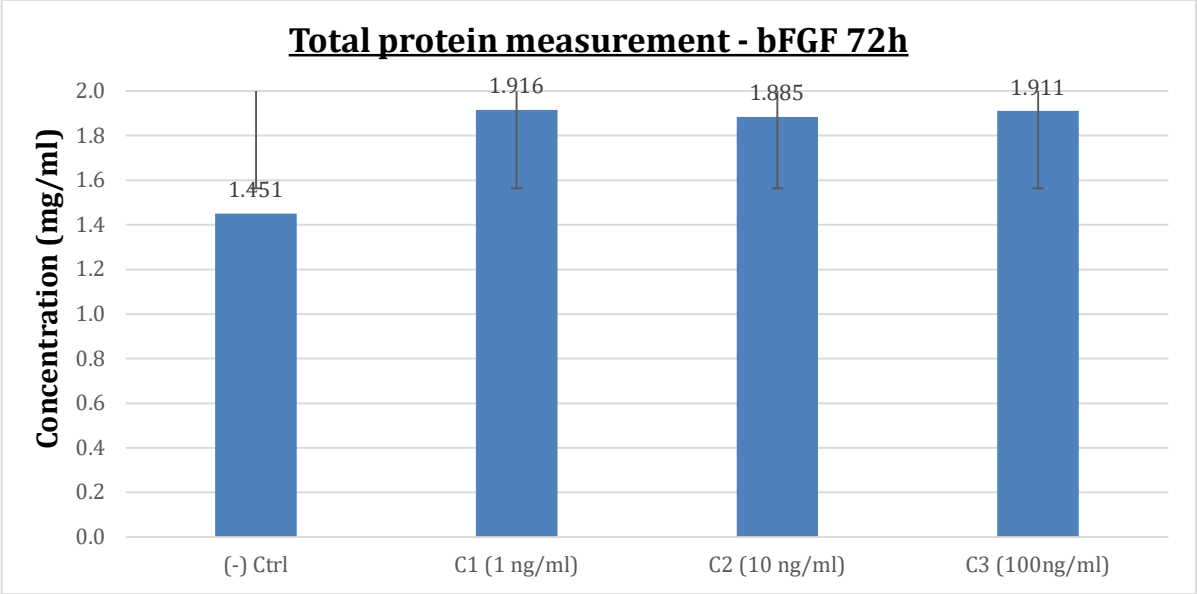

Figures 7. Total protein concentration of negative controls and basic fibroblast growth factor (bFGF) treated groups at 72 hours. Original optical density values to calculate the concentration were obtained through VERSAmax tunable microplate reader (Molecular Devices) and Softmax Pro 3.0 software. Microsoft Excel platform was used for data analysis and graph generation. The values correspond to the average sample concentration for each group. At 72h all treated groups had similar total protein content, ranging from 1.885 to 1.916 mg/ml whereas negative control group had an average of 1.45 mg/ml**.** The error bars represent the ±standard deviations based on three samples (n=3).

For the bFGF experiment, the total protein concentration increased in the pace of time without too much variation among the different treatments (**Figure 6**) for 24 and 48 hours. At 72 hours all the treated groups had similar total protein content (1.88 to 1.91 μg/μl in average) despite the bFGF treatment concentration. However, as shown in **Figure 7**, at 72h the untreated group appeared to have noticeably lower average total protein concentration (1.45 μg/μl) compared to the treated groups. The average total protein content for the treated groups was 1.916, 1.885 and 1.911 μg/μl for C1(1 ng/ml), C2(10 ng/ml) and C3 (100 ng/ml) treatments, respectively.

4.4 Western Blot for αSMA

Western blot aimed to examine the impact of TGFβ1 treatment (2 ng/ml) on αSMA expression. For that purpose, equal amount of total protein (15 μg) was loaded for both treated and untreated samples. Then, the untreated group displayed strong dark bands for αSMA expression whereas the TGFβ1 positive group displayed very bright bands in two of the three replicates. The third replicate had a clear band, indicating the presence of αSMA, but was weaker than the negative controls. The results of αSMA expression for the TGFβ1 treatments were inconclusive. The bands of the TGFβ1 group were very bright, potentially due to high amount of loaded protein.

Ponceau S was used to locate the blotted proteins on the PVDF membrane in order to assess equal protein loading and estimate the reliability of the results. Ponceau S staining was a reversible process, did not interfere with protein detection and did not dilute the protein content on the membrane. For the bFGF experiment, Ponceau S staining of PVDF membranes (**Figure 9**) ensured that equal amounts of total protein content were loaded on the gels for all groups and incubations, indicating that potential band intensity variation upon blocking with the antibody of interest, will correspond to the amount of targeted protein (αSMA).

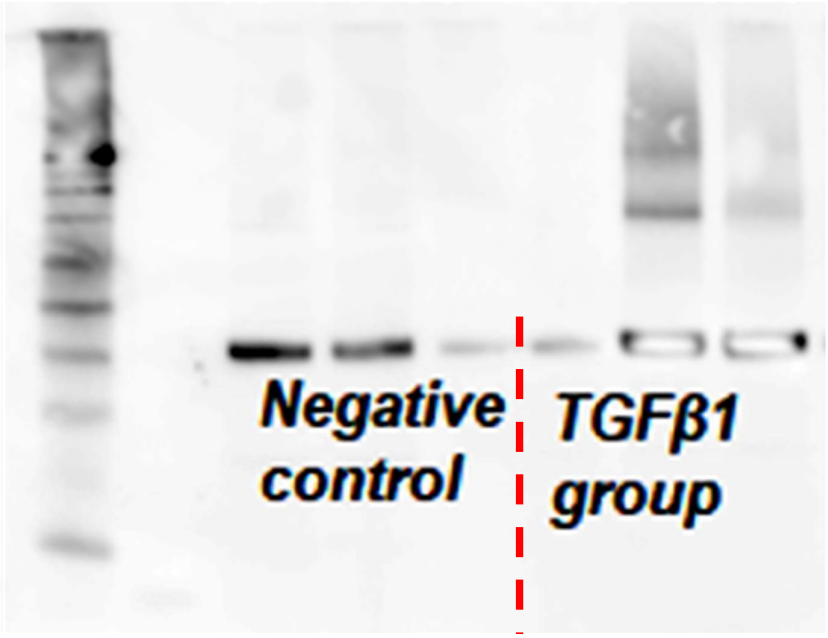

Figure 8. Imaged polyvinylidene fluoride (PVDF) membrane of alpha smooth muscle actin (αSMA) expression after 48 hours of transforming growth factor β1 (TGFβ1) treatment.The picture was exposed in Increment setting, on standard sensitivity for 120 seconds under LAS4000 imaging system by Fujifilm. Negative controls displayed strong and clear bands of αSMA whereas treated groups showed bands that were unclear, except one of the treated replicates that was clear but weaker than the negative controls.

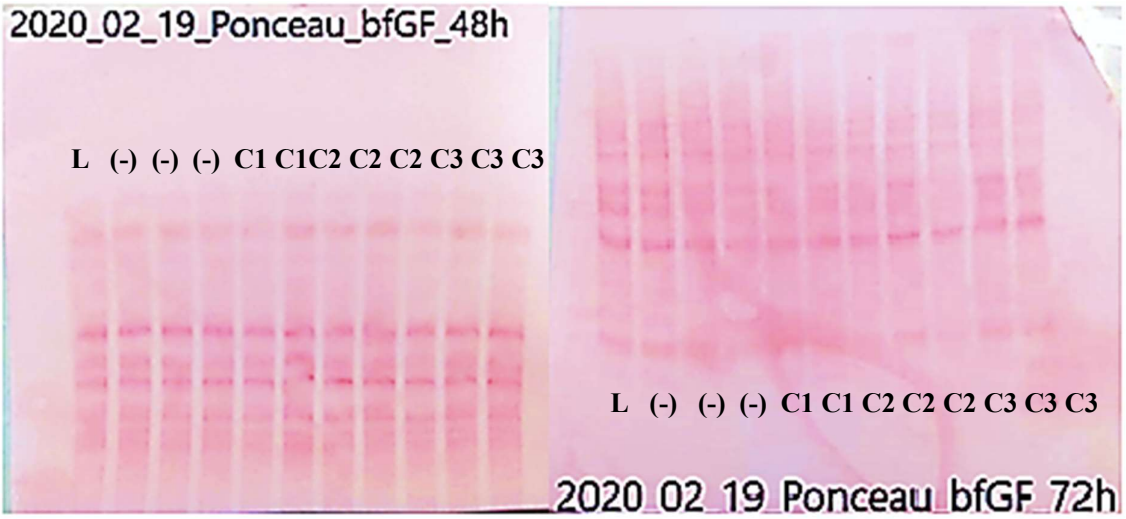

Figure 9. Ponceau S staining on PVDF Membranes of basic fibroblast growth factor (bFGF) treatments (48 and 72h), after blotting. Imaged with external camera. The band stains do not show a lot of variation, indicating that the gel was loaded with equal amount of protein.

After exposing the PVDF membranes, both the 48- and 72-hour incubations displayed stronger bands in the negative controls indicating that the expression of αSMA was the greatest when bFGF was absent. The expression of αSMA appears to decrease in all bFGF treated groups. As presented in **Figure 10**, αSMA was highly expressed on the untreated group, and although the band intensity weakens already in C1 group (1 ng/ml bFGF), the band intensity does not show any noticeable variation at C2 (10 ng/ml) C3 (100 ng/ml) treatments.

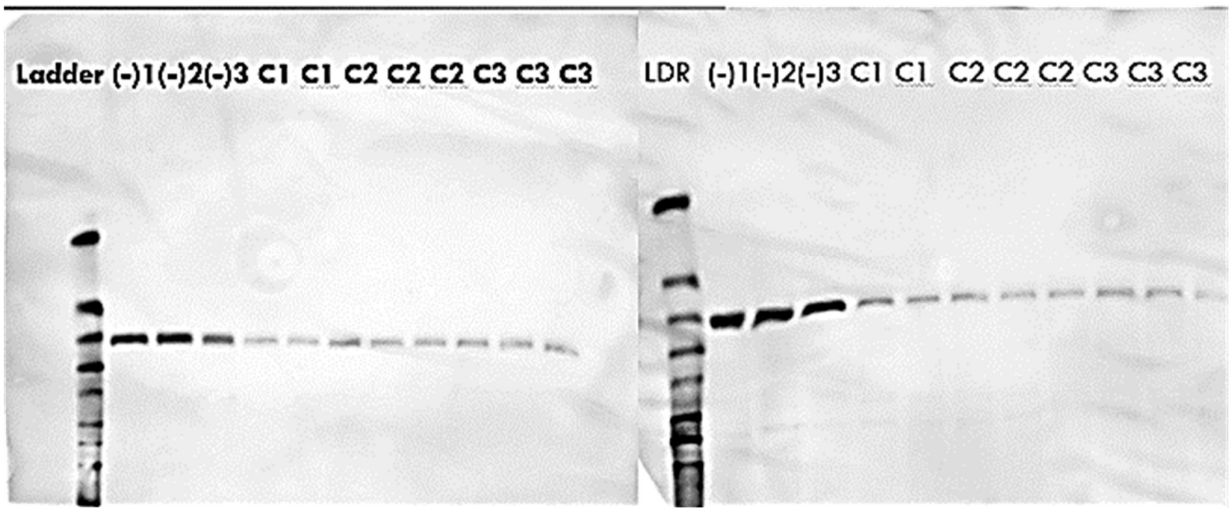

Figure 10. Imaged PVDF membranes of alpha smooth muscle actin (αSMA) expression after 48 (left) and 72 hours (right) of basic fibroblast growth factor (bFGF) treatment in three groups: C1=1 ng/ml, C2=10 ng/ml and C3=100 ng/ml. Negative control triplicates displayed next to the ladder. Left picture was exposed in Increment setting, on high sensitivity for 40 seconds. Right picture was exposed in Precision setting, on standard sensitivity, for 60 seconds. Both pictures were shot under LAS4000 imaging system by Fujifilm. All negative controls displayed the highest expression of αSMA. Among all replicates of treated groups, the αSMA expression was weaker compared to the untreated group and seemed to decline gradually as the bFGF treatment concentration increased.

4.5 Evaluation of S100A4 marker

4.5.1 Optimization

A wide range (1:50-1:3000) of S100A4 primary antibody dilutions, was tested to optimize the concentration in order to stain mouse tongue tumor tissues. The S100A4 primary antibody dilutions were 1:50 (**Figure 11B**), 1:250 (**Figure 11C**), 1:500 (**Figure 11D)**, 1:1000 (**Figure 11E)**, 1:1500 (**Figure 12C)**, 1:2000 (**Figure 12D)** and 1:3000 (**Figure 12E)**. Negative controls are presented on **Figure 11A and Figure 12A**. In smaller dilutions of primary antibody (**Figure 11-A to E**), the tissue was overstained both inside and outside of the tumor area. In lower concentrations of the primary antibody, heavy staining was still present, however the dilution 1:3000 (**Figure 12, image E**) had sufficient clarity to proceed on the next round of experiments. Therefore, the chosen dilution for the experiment was 1:3000.

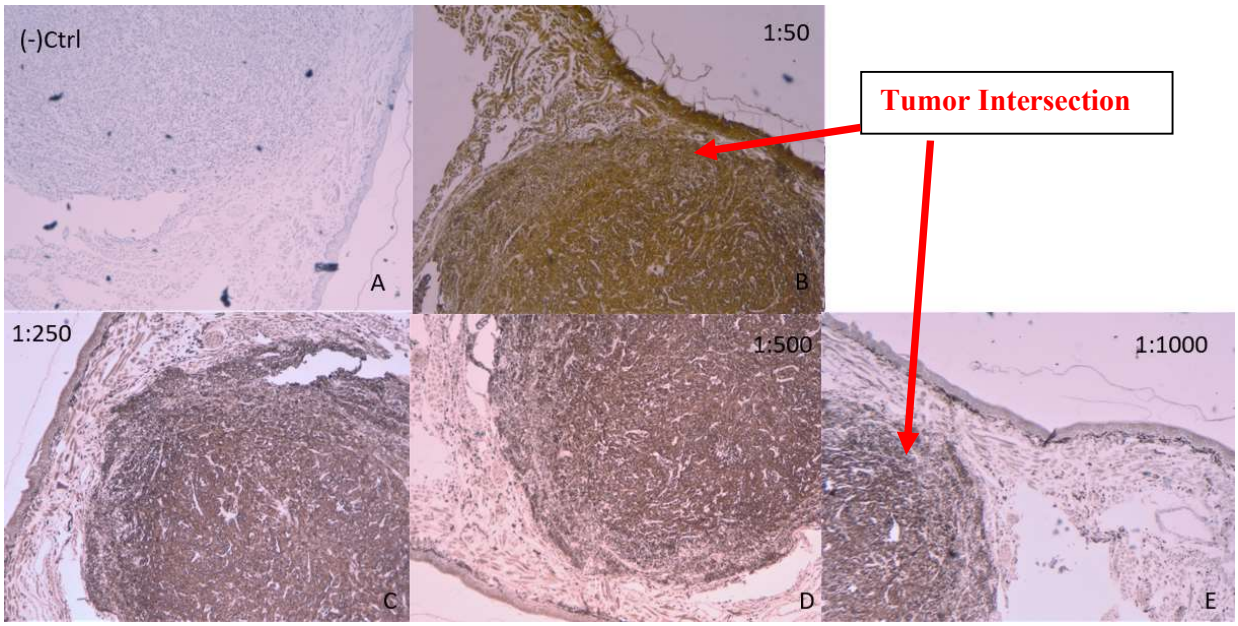

Figure 11. Immunohistochemistry on mouse tongue tissues for optimization of primary antibody dilutions. Range 1:50 (A) to 1:1000 (E). Magnified 4x. Shot under LEICA-DM2000 microscope with LAS V3.7 software. The whole range of antibody dilutions display excessive staining with heavy brown marks all over the tissue indicating that in this range of dilutions, S100A4 protein was present but it was not possible to identify the different cell types that express S100A4.

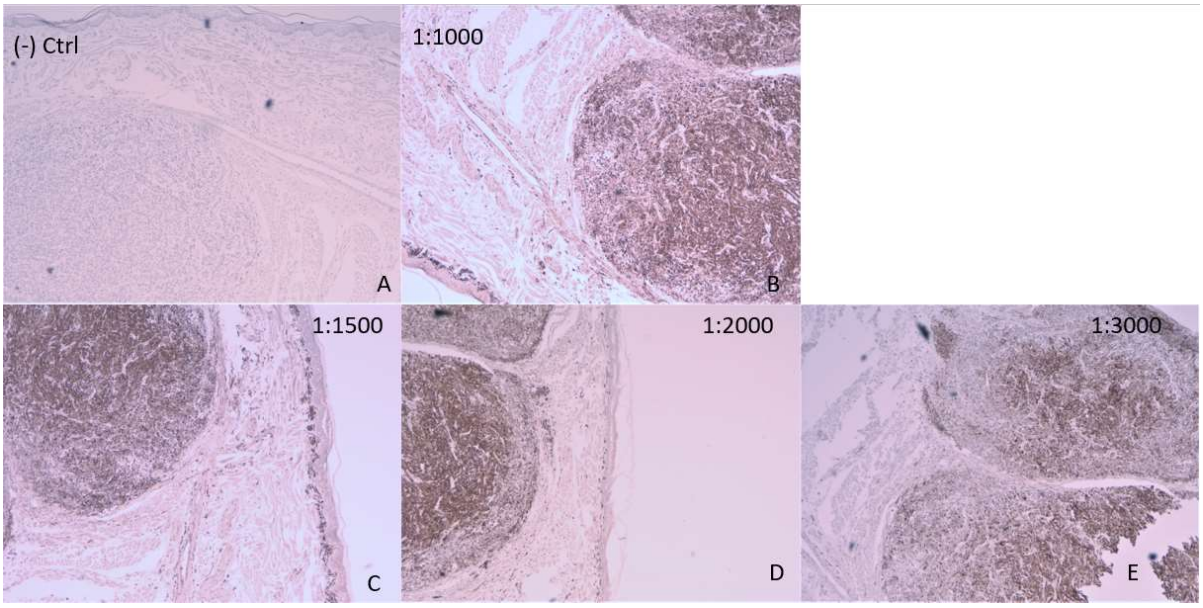

Figure 12. Immunohistochemistry on mouse tongue tissues for optimization of primary antibody dilutions. Range 1:1000 (A) to 1:3000 (E). Pictures shot under LEICA-DM2000 microscope with LAS V3.7 software . Magnified 4x. The present set of antibody dilutions appeared to have less unspecific staining compared to smaller dilutions (**Figure 11**) however, in pictures A-D there is still some fair staining on the insets of the tissue. Picture E shows a more specific stained area inside the tumor, indicating that 1:3000 is an acceptable antibody dilution to proceed further.

4.5.2 Positive tissues staining

Even though the optimal primary antibody dilution was chosen (1:3000) there was a lot of staining both inside and outside of the tumor area (**Figure 13**) for the tissues (D, E, F). The tissues were imaged in 4x magnification (**Figure 14**), where there is extensive stain inside the tumor as well as around the intersection where some fibroblasts may reside. There is also stain in the rest of the tongue tissue (insets) around the tongue muscle. The stain was precise on targeting the S100A4 protein areas, but it is not clear whether the rest of stained areas correspond to S100A4 expression coming from cancer cells or not. Therefore, S100A4 did not seem to be an ideal marker for OSCC.

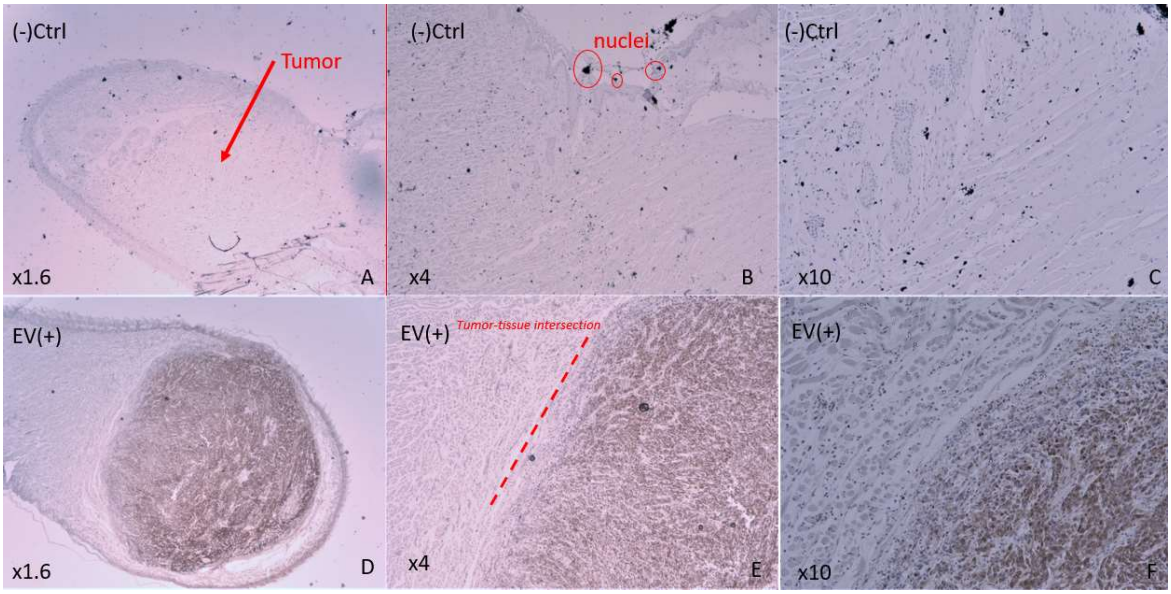

Figure 13. Immunohistochemistry for S100A4 on mouse tongue tissues (D, E, F) compared to the negative controls (A, B, C). Pictures imaged through LEICA-DM2000 microscope with LAS V3.7 software . Magnified 1.6x (left), 4x (center) and 10x times (right). Negative controls did not display any stain on the tumor. Nuclei were stained in dark blue color by the Hematoxylin. The positive tissues had a lot of stain both within the tumor and the rest of the tissue.

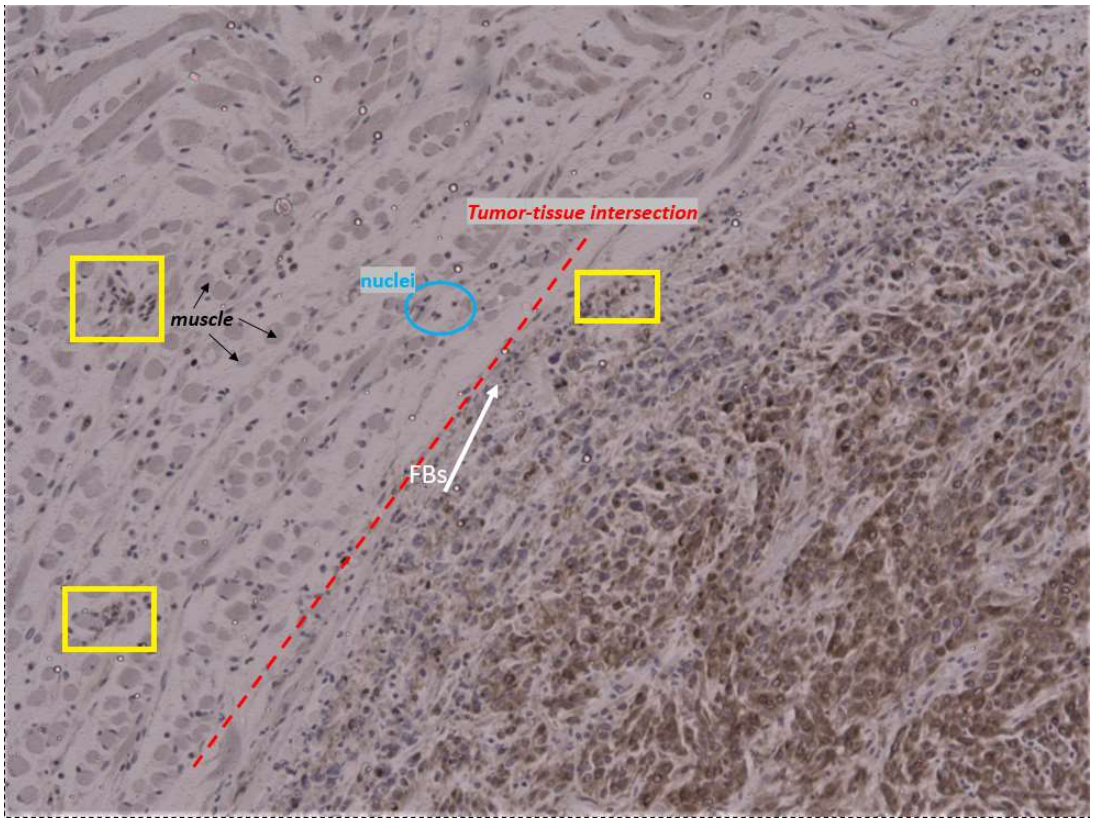

Figure 14. 10x magnified image of positive mouse tongue tissue, stained for S100A4. White arrow displays the presence of fibroblasts around the tumor-tissue intersection (red line). In the blue circle there are nuclei, stained blue by hematoxylin oxidation. Black arrows marks reflect tongue muscles and yellow squares highlight some unspecific staining in and out of the tumor area. Image taken under LEICA-DM2000 microscope with LAS V3.7 software.

5 Discussion

5.1 Fibroblast activation with TGFβ1

TGFβ1 is known to promote proliferation (Liu et al., 2016). In this current study a fixed treatment concentration (2 ng/ml) was used across 24, 48 and 72h. In 24 and 48h the TGFβ1 treated cells proliferated faster and displayed fiber-like morphology, compared to their negative controls (**Figure 3**). At 72h both treated and untreated cells were confluent without any notable difference, suggesting that TGFβ1 had little to no impact after 72h in morphology. The samples undergone total protein quantification and as displayed in **Figure 5b**, the TGFβ1 treated cells showed higher total protein content compared to the negative controls at all incubations (24, 48, 72h). Additionally, the total protein content for 72h set (both negative and treated cells) was noticeably high compared to the 48h incubation. Thus, the total protein content for 72h groups reflected high proliferation and complimented the microscopy results (**Figure 3**) for 72h being a confluency point for fibroblasts. All things considered, these results indicated that TGFβ1 seems to enhance proliferation, though probably not statistically significant. This was seen in both morphology (cell images) and total protein concentrations.

5.2 Fibroblast activation with bFGF

Basic fibroblast growth factor (bFGF) is reported to increase proliferation (Makino et al., 2009) and contribute to wound healing, cancer development, angiogenesis and metastasis. In this project, different concentrations (1-100 ng/ml) of bFGF treatments were tested to observe proliferation and morphology differences. In the first 24 hours, there was an effect of bFGF in proliferation and morphology. In particular, the highest bFGF treatment group (C3 = 100 ng/ml) displayed increased proliferation and more defined fiber-like morphology compared to the negative group. As seen in **Figure 4**, the treated groups C1 (1 ng/ml) and C2 (10 ng/ml) did not show any noticeable difference, suggesting that bFGF can increase proliferation within 24 hours when present in high concentration. Given that in 48 and 72h all groups

(treated and untreated) were very dense with prominent fiber structure, bFGF didn't seem to have a concentration-depended effect on cell number after 24 hours. Total protein quantification on the samples seems to back up this conclusion. As presented on **Figure 7b**, at 72h all three treated groups seem to have very similar total protein content (range 1.885-1.916 μg/μl) whereas the negative control at 72h had an average value of 1.45 μg/μl, suggesting that at 72h, bFGF enhances proliferation at any concentration.

5.3 Western Blot for αSMA

5.4 TGFβ1 treated fibroblasts

Literature has linked TGFβ1 to increased expression of αSMA (Malmström et al., 2014), although the regulation mechanism appears to be rather complex as it involves the activation of multiple signaling pathways that work synergistically (Sebe et al., 2008). Since TGFβ1 enhances proliferation and αSMA expression, a fixed concentration of 2 ng/ml was used for the treated group. The hypothesis was that TGFβ1 treated fibroblasts would display increased αSMA expression. In action, our findings partially agreed to the literature (Satish et al., 2011). We observed increased proliferation on treated groups compared to the controls, especially at 24 and 48h (**Figure 3**). Furthermore, the total protein content at **Figure 5b** also reflected a constantly higher total protein content on the treated groups compared to their respective negative controls. The Western Blot analysis for the TGFβ1 samples have been an active challenge for this project. There was a lot of troubleshooting and optimization required in order to obtain a presentable result of the PVDF membrane. As seen in **Figure 8**, the negative controls seemed to have some αSMA expression and the TGFβ1 treated fibroblasts were expected to display a stronger band than the controls. However, after multiple attempts to expose the membrane, the TGFβ1 technical replicates kept showing a very bright band. That might be a consequence of very high protein load but since there was no Ponceau S staining available to assess equal protein, the results are inconclusive.

5.5 bFGF treated fibroblasts

Previous research on the field suggests that bFGF downregulates the expression of αSMA (Ishiguro et al. 2009; Shinde et al. 2016). The hypothesis of this master project was to test and potentially confirm the inhibiting effect of bFGF. The objective also aimed to examine the effect of bFGF treated fibroblasts on αSMA expression, among different bFGF concentrations (1, 10 and 100 ng/ml). After analyzing the negative controls and the three different treatments on 24, 48 and 72h, the samples undergone Western Blotting. The 48h and 72h membrane

results shown in **Figure 10**, suggest that αSMA expression is indeed the highest on negative controls, both at 48 and 72h incubations. The bands corresponding to αSMA in the treated groups appear to be much weaker than the bands of untreated groups, however, there was no visual difference of αSMA expression among the treated groups, C1 (1 ng/ml), C2 (10 ng/ml) and C3 (100 ng/ml bFGF treatment). These findings agree with the literature as Shinde et al. (2016), also observed decrease in αSMA when they treated fibroblasts with 50ng/ml of bFGF. It seems that although bFGF reduces αSMA at any concentration there is no gradual decrease of αSMA as the bFGF treatment concentration increases. However, the results themselves were not very clear and require further validation.

5.6 Assessment of S100A4 protein as OSCC biomarker

The third and last hypothesis of this project was the assessment of S100A4 as a good biomarker for OSCC. For that purpose, two rounds of optimization took place to test a wide range of primary antibody dilutions from 1:50 up to 1:3000. The smaller dilutions were too intense and unspecific as presented in **Figures 11** and **12**. The highest dilution (1:3000) appeared to be decent on the optimization rounds and was chosen for testing on mouse tongue sections with tumor. Natarajan et al. (2014) discuss about S100A4 overexpression being correlated to lymph node metastasis on OSCC and suggest that S100A4 could be a good prognostic biomarker. Reckenbeil et al. (2016) also agree that S100A4 can be a promising target for OSCC. In this project, the results were contradictive to the mentioned suggestions. Even at the highest dilution (1:3000) that was supposed to increase the accuracy of the staining, the findings implied that S100A4 might not be very efficient biomarker. Although the tumor area was significantly stained, there was a lot of positive staining distributed on the intersection between tumor and normal tissue (**Figure 14**), on the insets as well as the circumference of the tissue where fibroblasts may reside. Lastly, there was also some staining around the tongue muscles, therefore S100A4 biomarker did not appear to be reliable for specific staining of cancer cells because the positive S100A4 may be secreted from normal cells as well.

6 Conclusions

This project aimed to examine three hypotheses. First, *in vitro* activation of fibroblasts with TGFβ1 and bFGF that was successful. The cells were cultured in TGFβ1 and bFGF treatments for 24, 28 and 72h. Both TGFβ1 and bFGF seem to increase proliferation. In a fixed TGFβ1 concentration of 2 ng/ml there was a noticeable difference between treated and

negative controls in 24h and 48h whereas at 72h TGFβ1 seemed to have no impact as both treated and untreated groups were equally confluent, elongated with prominent actin stress fibers. The bFGF experiment tested three treatment concentrations of 1, 10 and 100 ng/ml respectively. Both microscopy and total protein quantification show that in the first 24 hours, bFGF had a visual effect on the highest concentration treatment (100 ng/ml) while at 48h and 72h the cells were very dense with stress fibers at all concentrations. Thus, bFGF seems to increase proliferation and promote the activated fibroblast morphology at any concentration after 48h hours of treatment.

Second hypothesis was that TGFβ1 increases αSMA expression while bFGF reduces it. The literature suggests that TGFβ1 enhances αSMA, however the results of this experiment are considered inconclusive as the Western blot analysis for the treated group displayed very bright bands that could not be assessed. Previous research on the field claims that bFGF downregulates αSMA. The experiment confirmed that untreated groups displayed higher αSMA expression compared to all bFGF treatments. The band intensity was very similar among the different bFGF treatments. Therefore, it was challenging to assess weither αSMA expression may decline as the bFGF concentration increases among the treatment groups or not. Given that this experiment was tested only once, among three technical replicates, no conclusion can be made for a concentration-dependent effect of bFGF on αSMA expression. Our findings support that bFGF treatment reduces αSMA at any concentration, compared to untreated fibroblasts.

Lastly, the third hypothesis considers S100A4 to be a reliable biomarker for OSCC. There is a lot of research highlighting the correlation between S100A4 overexpression and lymph node metastasis on OSCC while claiming that S100A4 is a promising biomarker. Upon optimization, a very high dilution (1:3000) of S100A4 was used to increase the accuracy of the staining. The findings of this project are contradictive since S100A4 showed a lot of staining in many areas outside of the tumor, like tumor-normal tissue intersection, insets, tongue muscles and tongue section circumference. The cancer cells were certainly stained heavily but it was unclear if the stained areas outside of the tumor correspond to cancer cells since S100A4 can also be secreted by fibroblasts. Therefore, S100A4 seems to be a less efficient biomarker for OSCC. Assessing the literature, the proteins of S100 family appear to be positively correlated to OSCC progression and metastasis. Consequently, other S100 proteins could be a good target for biomarker testing research, as in the example of S100A8 that seems to be a sensitive biomarker for OSCC diagnosis (Jou., et al., 2014).

7 References

Bussard, K. M., Spaeth, E., Mutkus, L. A., and Stumpf, K. 2017. Mesenchymal stem cell transition to tumor-associated stromal cells contributes to cancer progression. In the book: *Mesenchymal Stromal Cells as Tumor Stromal Modulators*, pp. 253–273, doi: 10.1016/b978-0-12-803102-5.00011-2

Desjardins-Park, H. E., Foster, D. and Longaker, M. T. 2018. Fibroblasts and Wound Healing: an Update. *Regenerative Medicine*, vol. 13, no. 5, pp. 491–495., doi:10.2217/rme-2018-0073.

Desmoulière, A., Geinoz, A., Gabbiani, F., and Gabbiani, G. 1993. Transforming growth factor-beta 1 induces alpha-smooth muscle actin expression in granulation tissue myofibroblasts and in quiescent and growing cultured fibroblasts. *The Journal of Cell Biology* 122*(*1): 103–111. https://doi.org/10.1083/jcb.122.1.103

Elmusrati, A. A., Pilborough, A. E., Khurram, S. A., and Lambert, D. W. 2017. Cancer-associated fibroblasts promote bone invasion in oral squamous cell carcinoma. *British Journal of Cancer* 117(6): 867-875, doi:10.1038/bjc.2017.239

Fei, F., Liu, K., Li, C., Du, J., Wei, Z., Li, B., Li, Y., Zhang, Y. And Zhang, S. 2020. Molecular Mechanisms by Which S100A4 Regulates the Migration and Invasion of PGCCs With Their Daughter Cells in Human Colorectal Cancer. *Frontiers in Oncology*, vol. 10, doi:10.3389/fonc.2020.00182.

Foster, D. S., Jones, R. E., Random, R. C., Longaker, M. T. and Norton, J. A. 2018. The Evolving Relationship of Wound Healing and Tumor Stroma. *JCI Insight*, American Society for Clinical Investigation, www.ncbi.nlm.nih.gov/pmc/articles/PMC6237224/.

Gomes, A., Teixeira, C., Ferraz, R., Prudencio, C. and Gomes, S. 2017. Wound-Healing Peptides for Treatment of Chronic Diabetic Foot Ulcers and Other Infected Skin Injuries. *Molecules,* vol. 22, no. 10, p. 1743., doi:10.3390/molecules22101743.

Sasahira, T. and Kirita, T. 2018. Hallmarks of Cancer-Related Newly Prognostic Factors of Oral Squamous Cell Carcinoma. *International Journal of Molecular Sciences*, vol. 19, no. 8, p. 2413., doi:10.3390/ijms19082413.

Hase, T., Kawashiri, S., Tanaka, A., Nozaki, S., Noguchi, N., Kato, K., Nakaya, H. and Nakagawa, K. 2006. Correlation of Basic Fibroblast Growth Factor Expression with the Invasion and the Prognosis of Oral Squamous Cell Carcinoma. *Wiley Online Library*, John Wiley & Sons, Ltd, doi:10.1111/j.1600-0714.2006.00397.x.

Higashino, N., Koma, Y. i., Hosono, M., Takase, N., Okamoto, M., Kodaira, H., Nishio, M., Shigeoka, M., Kakeji, Y. and Yokozaki, H. 2019. Fibroblast Activation Protein-Positive Fibroblasts Promote Tumor Progression through Secretion of CCL2 and Interleukin-6 in Esophageal Squamous Cell Carcinoma. *Laboratory Investigation*, vol. 99, no. 6, 2019, pp. 777–792., doi:10.1038/s41374-018-0185-6.

Ishiguro, S., Akasaka, Y., Kiguchi, H., Suzuki, T., Imaizumi, R., Ishikawa, Y., Ito, K. and Ishii, T. 2009. Basic Fibroblast Growth Factor Induces down-Regulation of Alpha-Smooth Muscle Actin and Reduction of Myofibroblast Areas in Open Skin Wounds. *Wound Repair and Regeneration: Official Publication of the Wound Healing Society [and] the European Tissue Repair Society*, U.S. National Library of Medicine, pubmed.ncbi.nlm.nih.gov/19614927/.

Jou, Y. J., Hua, C. H., Lin, C. D., Lai, C. H., Huang, S. H., Tsai, M. H., Kao, J. Y. and Lin, C. W. 2014. S100A8 As Potential Salivary Biomarker of Oral Squamous Cell Carcinoma Using NanoLC–MS/MS. *Clinica Chimica Acta*, vol. 436, pp. 121–129., doi: 10.1016/j.cca.2014.05.009.

Kim, H. S. 1998. Assignment of the Human Basic Fibroblast Growth Factor Gene FGF2 to Chromosome 4 Band q26 by Radiation Hybrid Mapping. *Cytogenetic and Genome Research*, vol. 83, no. 1-2, pp. 73–73., doi:10.1159/000015129.

Lee, K. Y. 2019. M1 and M2 polarization of macrophages: a mini-review. *Medical Biological Science and Engineering*, 2(1), 1–5. https://doi.org/10.30579/mbse.2019.2.1.1

Li, Z. H. and Bresnick, A. R. 2006. The S100A4 Metastasis Factor Regulates Cellular Motility via a Direct Interaction with Myosin-IIA. *Cancer Research*, vol. 66, no. 10, pp. 5173–5180. doi: 10.1158/0008-5472.can-05-3087

Liu, Y., Li, Y., Li, N. Teng, W., Wang, M., Zhang, W. and Xiao, Z. 2016. TGF-β1 promotes scar fibroblasts proliferation and transdifferentiation via up-regulating MicroRNA-21. *Scientific Reports*, Rep 6, 32231. https://doi.org/10.1038/srep32231

Makino, T., Jinnin, M., Muchemwa, F. C., Fukushima, S., Nishi, H. K., Moriya, C., Igata. T., Fujisawa, A., Johno, T. and Ihn, H. 2009. Basic Fibroblast Growth Factor Stimulates the Proliferation of Human Dermal Fibroblasts via the ERK1/2 and JNK Pathways. *British Journal of Dermatology*, vol. 162, no. 4, pp. 717–723., doi:10.1111/j.1365-2133.2009.09581.x.

Malmström, J., Lindberg, H., Lindberg, C., Bratt, C., Wieslander, E., Delander, E. L., Särnstrand, B., Burns, J. S., Larsen, M. P., Fey, S. and Marko, V. G. 2004. Transforming Growth Factor-β1 Specifically Induce Proteins Involved in the Myofibroblast Contractile Apparatus. *Molecular & Cellular Proteomics*, American Society for Biochemistry and Molecular Biology. www.mcponline.org/content/3/5/466

Maroni, D. and Davis, J. S. 2012. Transforming Growth Factor Beta 1 Stimulates Profibrotic Activities of Luteal Fibroblasts in Cows1. *Biology of Reproduction*, vol. 87, no. 5. doi:10.1095/biolreprod.112.100735.

Nakamichi, M., Fukasawa, Y. A., Fujisawa, C., Mikami, T., Onishi, K. and Akasaka, Y. 2016. Basic Fibroblast Growth Factor Induces Angiogenic Properties of Fibrocytes to Stimulate Vascular Formation during Wound Healing. *The American Journal of Pathology*, Volume 186, Issue 12, pp. 3203-3216, ISSN 0002-9440. https://doi.org/10.1016/j.ajpath.2016.08.015

Natarajan, J., Hunter, K., Mutalik, V. S. and Radhakrishnan, R. 2014. Overexpression of S100A4 as a biomarker of metastasis and recurrence in oral squamous cell

carcinoma. *Journal of applied oral science*: 22(5), 426–433. https://doi.org/10.1590/1678-775720140133

Rauch, C., Feifel, E., Amann, E. M., Spötl, H. P., Schennach, H., Pfaller, W. and Gstraunthaler G. Alternatives to the Use of Fetal Bovine Serum: Human Platelet Lysates as a Serum Substitute in Cell Culture Media. 2011. *ALTEX* ; 28(4): 305-16. Doi: 10.14573/altex.2011.4.305.

Reckenbeil, J., Kraus, D., Probstmeier, R., Allam, J. P., Novak, N., Frentzen, M., Martini, M., Wenghoefer, M. and Winter, J. 2016. Cellular Distribution and Gene Expression Pattern of Metastasin (S100A4), Calgranulin A (S100A8), and Calgranulin B (S100A9) in Oral Lesions as Markers for Molecular Pathology. *Cancer Investigation*, 34:6, 246-254, DOI: 10.1080/07357907.2016.1186172

Sahai, E., Astsaturov, I., Cukierman, E., DeNardo, D. G., Egeblad, M., Evans, R. M., Fearon, D., Greten, F. R., Hingorani, S. R., Hunter, T., Hynes, R. O., Jain, R. K., Janowich, T., Jorgensen, C., Kimmelman, A. C., Kolonin, M. G., Maki, R. G., Powers, S., Puré, E., Ramirez, D. C., Shouval, R. S., Sherman, M. H., Stewart, S., Tisty, T. D., Tuveson, D. A., Watt, F. M., Weaver, V., Weeraratna, A. T. and Werb, Z. 2020. A framework for advancing our understanding of cancer-associated fibroblasts. *Nature Reviews Cancer:* 20, 174–186. https://doi.org/10.1038/s41568-019-0238-1

Santi, A., Caselli, A., Ranaldi, F., Paoli, P., Mugnaioni, C., Michelucci, E. and Cirri, P. 2015. Cancer Associated Fibroblasts Transfer Lipids and Proteins to Cancer Cells through Cargo Vesicles Supporting Tumor Growth. *Biochimica Et Biophysica Acta (BBA) – Molecular Cell Research*, Elsevier: vol. 1853, no.12, pp. 3211-3223. Doi:10.1016/j.bbamcr.2015.09.013.

Santos, H. B. P., Santos, T.K.G., Paz, A. R., Cavalcanti, Y. W., Weege-Nonaka, C. F., Godoy, G. P. and Alvez, P. M. 2016. Clinical Findings and Risk Factors to Oral Squamous Cell Carcinoma in Young Patients: A 12-Year Retrospective Analysis. Medicina Oral, *Patologia Oral y Cirugia Bucal, Medicina Oral S.L.* www.ncbi.nlm.nih.gov/pmc/articles/PMC4788792/.

Satish, L., Gallo, P. H., Baratz, M. E., Johnson, S. and Kathju, S. 2011. Reversal of TGF-β1 Stimulation of α-Smooth Muscle Actin and Extracellular Matrix Components by Cyclic AMP in Dupuytren's-Derived Fibroblasts. BMC Musculoskeletal Disorders, *BioMed Central*, vol. 12, no. 113, doi: 10.1186/1471-2474-12-113

Sebe, A., Leivonen, S. K., Fintha, A., Masszi, A., Rosivall, L., Kähäri, V. M. and Mucsi, I. 2008. Transforming Growth Factor- -Induced Alpha-Smooth Muscle Cell Actin Expression in Renal Proximal Tubular Cells Is Regulated by p38 Mitogen-Activated Protein Kinase, Extracellular Signal-Regulated Protein kinase1,2 and the Smad Signalling during Epithelial-Myofibroblast Transdifferentiation. *Nephrology Dialysis Transplantation*, vol. 23, no. 5, pp. 1537–1545., doi:10.1093/ndt/gfm789.

Sherbet, G. V. 2017. S100A4 Has Potential Benefits as a Therapeutic Target. *Molecular Approach to Cancer Management*, 211–221. Doi: 10.1016/b978-0-12-812896-1.00025-8

Shield, K. D., Ferlay, J., Jemal, A., Sankaranarayanan, R., Chaturvedi, A. K., Bray, F. and Soerjomataram, I. 2016. The Global Incidence of Lip, Oral Cavity, and Pharyngeal Cancers by Subsite in 2012. *American Cancer Society Journals*, American Cancer Society, Doi:10.3322/caac.21384

Shinde, V. A., Humeres, C. and Frangogiannis, N. G. 2017. The Role of α-Smooth Muscle Actin in Fibroblast-Mediated Matrix Contraction and Remodeling. *Biochimica Et Biophysica Acta (BBA) - Molecular Basis of Disease*, Elsevier, vol. 1863, no.1, pp. 298-309, doi: 10.1016/j.bbadis.2016.11.006.

Song, S., Wientjes, M. G., Gan, Y. and Au, J.L. 2000. Fibroblast growth factors: An epigenetic mechanism of broad spectrum resistance to anticancer drugs. *Proceedings of the National Academy of Sciences of America (PNAS)*; vol. 97, no.15, pp. 8658–8663, doi:10.1073/pnas.140210697

Weinberg, R. A. (2015). *The biology of cancer: 2nd edition*. Moore Park, CA: Content Technologies.

Wetting, H. L., Olsen, E. H., Magnussen, S., Rikardsen, O., Steigen, S. E., Sundkvist, E., Loennechen, T., Kanapathipillai, P., Kildasen, H., Winberg, J. O., Hansel, U. H. and Svineng, G. 2011. S100A4 Expression in Xenograft Tumors of Human Carcinoma Cell Lines Is Induced by the Tumor Microenvironment. *The American Journal of Pathology*, vol. 178, no. 5, pp. 2389–2396., doi:10.1016/j.ajpath.2011.01.022.

Yavuz, B. G., Gunaydin, G., Gedik, M. E., Kosemehmetoglu, K., Karakoc, D., Ozgur, F. and Guc, D. 2019. Cancer Associated Fibroblasts Sculpt Tumor Microenvironment by Recruiting Monocytes and Inducing Immunosuppressive PD-1+ TAMs. *Scientific Reports*, vol. 9, no. 1, 2019, doi:10.1038/s41598-019-39553-z.

Websites/Data bases:

1. ATCC – LGC Standards, Norway (MRC5 vender) : https://www.lgcstandards-atcc.org/products/all/CCL-171.aspx?geo_country=no#characteristics
2. Global Cancer Observatory (GLOBOCAN) : https://gco.iarc.fr/today/data/factsheets/populations/900-world-fact-sheets.pdf
3. Surveillance, Epidemiology and End Rersults Program- (SEER): https://seer.cancer.gov/statfacts/html/oralcav.html

8 Supplements

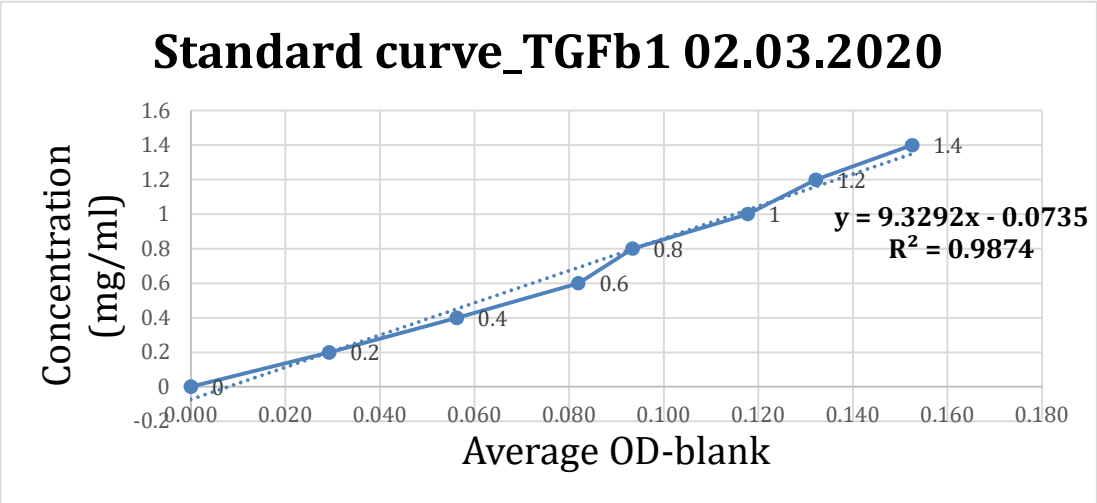

Supplementary figure 1. The standard curve was obtained by total protein measurement of BSA standard dilutions in order to extrapolate the calibrated concentration formula on the transforming growth factor beta 1 (TGFβ1) samples (24, 48 and 72h). The average optical density minus the blank was converted into total protein concentration based on the formula above. The corresponding graph of sample concentrations (**Figure 5**) is shown at the results section.

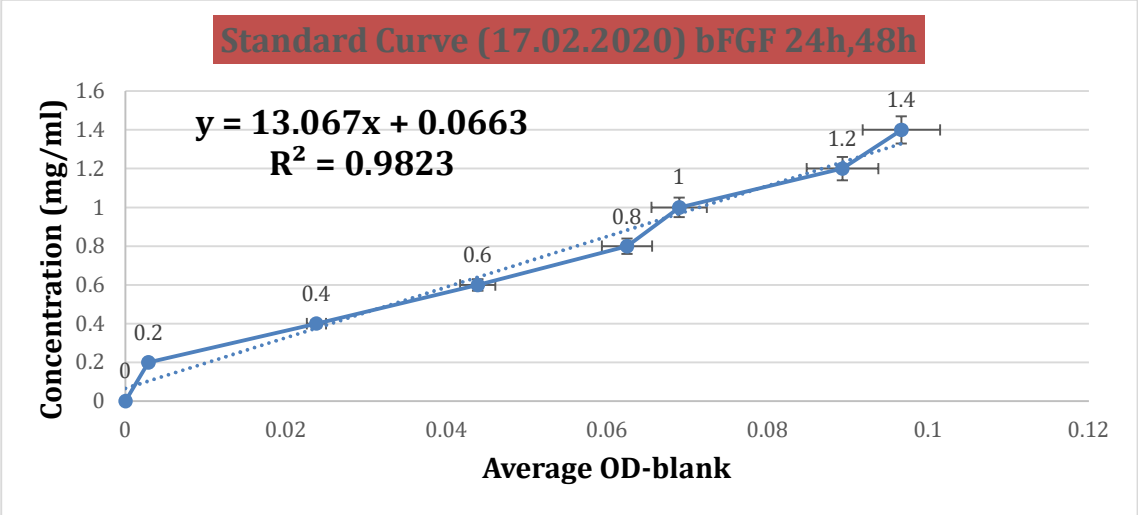

Supplementary figure 2. The standard curve was obtained by total protein measurement of BSA standard dilutions in order to extrapolate the calibrated concentration formula on the bFGF samples (24 and 48h). The average optical density minus the blank was converted into total protein concentration based on the formula above. The corresponding graph of sample concentrations (**Figure 6**) is shown at the results section.

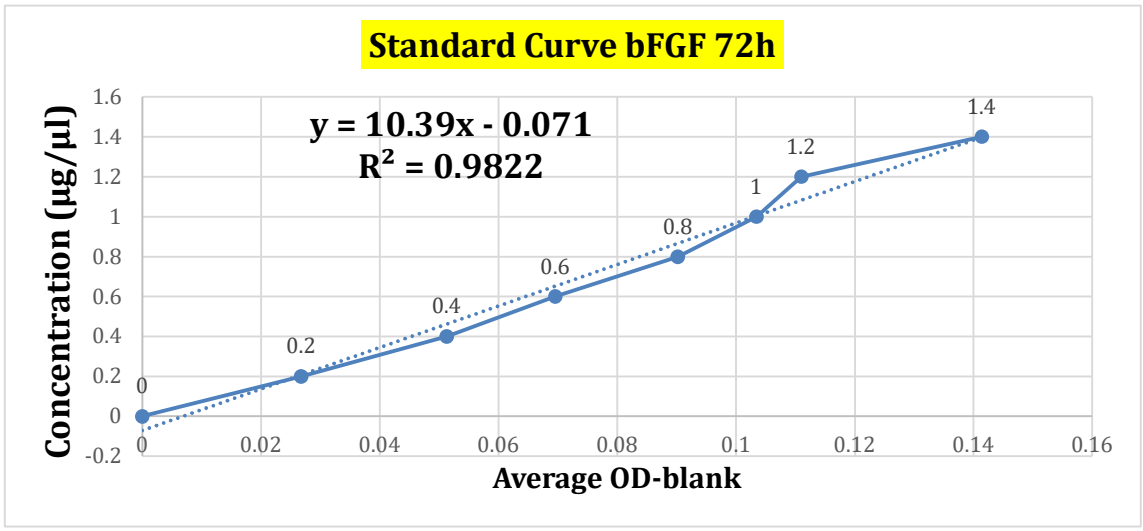

Supplementary figure 3. The standard curve was obtained by total protein measurement of BSA standard dilutions to extrapolate the calibrated concentration formula on the bFGF samples (72h). The average optical density minus the blank was converted into total protein concentration based on the formula above. The corresponding graph of sample concentrations (**Figure 7**) is shown at the results section.